

AD-A130 660

MECHANISM SWITCHING AND TRAPPING OF TRIPLET-TRIPLET
ENERGY TRANSFER IN AN... (U) CALIFORNIA UNIV LOS ANGELES
DEPT OF CHEMISTRY J R MORGAN ET AL. 15 JUL 83 TR-43
N00014-75-C-0602

1/1

UNCLASSIFIED

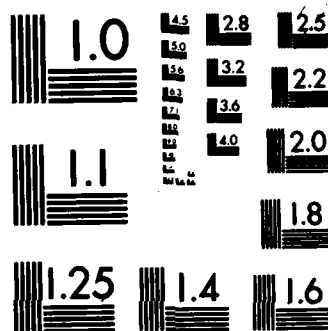
F/G 20/8

NL

END

FILED

100



MICROCOPY RESOLUTION TEST CHART
NATIONAL BUREAU OF STANDARDS-1963-A

12

AD A130660

OFFICE OF NAVAL RESEARCH

Contract N00014-75-C-0602

Task No. NR 056-498

TECHNICAL REPORT NO. 43

MECHANISM SWITCHING AND TRAPPING OF TRIPLET-TRIPLET
ENERGY TRANSFER IN AN ORIENTATIONALLY DISORDERED MOLECULAR SOLID

by

Jack R. Morgan and M. A. El-Sayed

Published J. Phys. Chem. 87, 2178 (1983)

University of California
Department of Chemistry and Biochemistry
Los Angeles, California 90024

July 15, 1983

STAMP
JUL 26 1983
A

Reproduction in whole or in part is permitted for
any purpose of the United States Government

This document has been approved for public release
and sale; its distribution is unlimited

DTIC FILE COPY

88 07 26 147

REPORT DOCUMENTATION PAGE		READ INSTRUCTIONS BEFORE COMPLETING FORM
1. REPORT NUMBER 43	2. GOVT ACCESSION NO. AD-A130660	3. RECIPIENT'S CATALOG NUMBER
4. TITLE (and Subtitle) Mechanism Switching and Trapping of Triplet-Triplet Energy Transfer in an Orientationally Disordered Molecular Solid		5. TYPE OF REPORT & PERIOD COVERED Interim Technical Report
		6. PERFORMING ORG. REPORT NUMBER
7. AUTHOR(s) Jack R. Morgan and M. A. El-Sayed		8. CONTRACT OR GRANT NUMBER(s) N00014-75-C-0602
9. PERFORMING ORGANIZATION NAME AND ADDRESS Regents of the University of California University of California, 405 Hilgard Ave. Los Angeles, CA 90024		10. PROGRAM ELEMENT, PROJECT, TASK AREA & WORK UNIT NUMBERS NR-056-498
11. CONTROLLING OFFICE NAME AND ADDRESS Office of Naval Research Chemistry Branch Arlington, Virginia 22217		12. REPORT DATE July 15, 1983
		13. NUMBER OF PAGES 42
14. MONITORING AGENCY NAME & ADDRESS (if different from Controlling Office) Office of Naval Research Branch Office 1030 East Green Street Pasadena, CA 91106		15. SECURITY CLASS. (of this report) Unclassified
		15a. DECLASSIFICATION/DOWNGRADING SCHEDULE
16. DISTRIBUTION STATEMENT (of this Report) This document has been approved for public release and sale; distribution of this document is unlimited.		
17. DISTRIBUTION STATEMENT (of the abstract entered in Block 20, if different from Report)		
18. SUPPLEMENTARY NOTES Published J. Phys. Chem. <u>87</u> , 2178 (1983)		
19. KEY WORDS (Continue on reverse side if necessary and identify by block number) Spectral diffusion Energy transfer Disordered solids		
20. ABSTRACT (Continue on reverse side if necessary and identify by block number) The separation between the ions or molecules in disordered solids varies at random. The optical transition energy could also vary over a wide range for the different molecules or ions in the solid resulting in a large inhomogeneous line width ($\Delta\nu_{inh}$). This allows energy transfer and spectral diffusion studies to be carried out between the same chemical species but at different local environments in these solids using lasers for excitation. Furthermore, when carried out at temperatures at which $kT \ll \Delta\nu_{inh}$, energy transfer becomes unidirectional, i.e.,		

to molecules or ions having transition energies equal or lower than the laser-excited-donors within the inhomogeneous profile. This allows studies on the dependence of the rate and mechanism of the energy transfer on the acceptor concentration (i.e., on donor-acceptor separation) to be carried out by simply changing the laser wavelength within the inhomogeneous profile. By analyzing the temporal behavior of the emission intensity of the pulsed-laser-excited set of molecules or ions (donors), the mechanism of the excitation transfer can be elucidated. These types of studies are carried out on the triplet-triplet energy transfer in a unique type of disordered solid, orientationally disordered molecular solids, e.g., 1-bromo,4-chloronaphthalene (BCN) neat solid. In this solid, the T_1-S_0 transition energy is inhomogeneously broadened with $\Delta\nu_{inh} = 64 \text{ cm}^{-1}$. The temporal behavior of the donor emission intensity can be described by a one-dimensional electronic exchange mechanism, expected for triplet-triplet energy transfer in this system, at laser wavelengths for which the mole fraction of acceptors is > 0.1 . At longer wavelengths, i.e., for acceptor mole fractions < 0.1 , the lower acceptors are on the average at distances for which the exchange mechanism becomes inefficient. This might explain the observation that at these wavelengths, the intensity temporal behavior can be described by the long range, three dimensional electric dipole-dipole mechanism. Not only the observed temporal behavior but also the quantitative acceptor concentration dependence results point out to the possibility of the mechanism switching for the triplet-triplet energy transfer process in this system.

At still larger donor-acceptor separation, the dipole-dipole mechanism becomes inefficient and the excitation energy becomes trapped on some of these randomly distributed sites. This allows radiative processes to be observed from these sites. As a result, the observed emission profile of the solid at low temperature is determined by the energy distribution of the emission of the trapping sites. Predictions based on these ideas are used and a fit is made to the 4.2 K observed phosphorescence profile of the BCN solid. The theoretical fit to the observed emission profile is discussed in terms of the possible energy transfer mechanism(s) discussed above.



SEARCHED		INDEXED	
SERIALIZED		FILED	
APR 1964			
FBI - NEW YORK			
A			

MECHANISM SWITCHING AND TRAPPING OF TRIPLET-TRIPLET ENERGY TRANSFER
IN AN ORIENTATIONALLY DISORDERED MOLECULAR SOLID

Jack R. Morgan and M. A. El Sayed
Department of Chemistry and Biochemistry
University of California
Los Angeles, California 90024

ABSTRACT

The separation between the ions or molecules in disordered solids varies at random. The optical transition energy could also vary over a wide range for the different molecules or ions in the solid resulting in a large inhomogeneous line width ($\Delta\nu_{inh}$). This allows energy transfer and spectral diffusion studies to be carried out between the same chemical species but at different local environments in these solids using lasers for excitation. Furthermore, when carried out at temperatures at which $kT \ll \Delta\nu_{inh}$, energy transfer becomes unidirectional, i.e. to molecules or ions having transition energies equal or lower than the laser-excited-donors within the inhomogeneous profile. This allows studies on the dependence of the rate and mechanism of the energy transfer on the acceptor concentration (i.e. on donor-acceptor separation) to be carried out by simply changing the laser wavelength within the inhomogeneous profile. By analyzing the temporal behavior of the emission intensity of the pulsed-laser-excited set of molecules or ions (donors), the mechanism of the excitation transfer can be elucidated. These types of studies are carried out on the triplet-triplet energy transfer in a unique type of disordered solid, orientationally disordered molecular solids, e.g. 1-bromo,4-chloronaphthalene (BCN) neat solid. In this solid, the T_1-S_0

transition energy is inhomogeneously broadened with $\Delta\nu_{inh} = 64 \text{ cm}^{-1}$. The temporal behavior of the donor emission intensity can be described by a one-dimensional electronic exchange mechanism, expected for triplet-triplet energy transfer in this system, at laser wavelengths for which the mole fraction of acceptors is > 0.1 . At longer wavelengths, i.e. for acceptor mole fractions < 0.1 , the lower energy acceptors are on the average at distances for which the exchange mechanism becomes inefficient. This might explain the observation that at these wavelengths, the intensity temporal behavior can be described by the long range, three dimensional electric dipole-dipole mechanism. Not only the observed temporal behavior but also the quantitative acceptor concentration dependence results point out to the possibility of the mechanism switching for the triplet-triplet energy transfer process in this system.

At still larger donor-acceptor separation, the dipole-dipole mechanism becomes inefficient and the excitation energy becomes trapped on some of these randomly distributed sites. This allows radiative processes to be observed from these sites. As a result, the observed emission profile of the solid at low temperature is determined by the energy distribution of the emission of the trapping sites. Predictions based on these ideas are used and a fit is made to the 4.2 K observed phosphorescence profile of the BCN solid. The theoretical fit to the observed emission profile is discussed in terms of the possible energy transfer mechanism(s) discussed above.

INTRODUCTION

In recent years, considerable interest has been shown in the optical properties of disordered solids, where the disorder can affect both the static and dynamic properties of electronic excitations. Research activities have been in three different types of these systems: the first is rare-earth ions in inorganic glasses^[1-5], second is protonated in deuterated isotopically mixed aromatic crystals^[6,7], and third (more recently) is orientationally disordered solids^[8-10] (ODS). The latter are molecular crystals which retain a high degree of translational correlation in terms of lattice positions of the center of mass and general molecular orientation but show a distribution of orientations with respect to substituent groups^[11]. An example of this type of disorder is the 1-bromo,4-chloronaphthalene (BCN) crystal^[12].

In all of the above systems, the disorder results from a random distribution of the separation between the different molecules or ions being studied. In the first and third systems, the separation as well as the transition energy of the molecules or ions of interest can also vary over a reasonably wide range. This gives rise to a relatively large inhomogeneous line width ($\Delta\nu_{inh}$) for these systems than in crystalline materials. In these solids, where the long range structural order of simple crystals is absent, not only the inhomogeneous width but also the homogeneous linewidth is found to be broader than in crystalline materials^[13,14]. The homogeneous broadening in glasses has been interpreted^[13-18] in terms of the 'two level system' model^[19,20] which postulates the existence of a

tunneling-type motion of atoms or molecules between two inequivalent minima. Both the inhomogeneous and homogeneous linewidths of Eu^{3+} in B_2O_3 glasses have been found^[21] to be sensitive to, and well correlated with chemical structural changes induced by the addition of Na_2O .

At higher impurity concentration in glasses, spectral diffusion among the impurity sites due to the nonradiative exchange of electronic excitation at temperatures where $kT > \Delta v_{\text{inh}}$ has been studied using time resolved fluorescence line narrowing techniques^[1-5]. The time dependence of the donor emission, which is sensitive to the coupling mechanism and disorder in donor-acceptor distances^[1,22-24], has been used^[2,3,5] to show that the transfer is dipolar in nature. Similar results are obtained with crystalline hosts, where a dipolar mechanism has also been found^[25].

In the case of molecular crystals, it is now accepted that triplet exciton transfer results from the electron exchange interaction^[26]. Energy transfer in pure crystals is well understood in terms of the exciton model^[26], where the electronic energy levels of the molecules become bands in the crystal. In the isotopic mixed molecular (disordered) crystals, the large increase in the energy transfer efficiency at some critical trap concentration^[6,7] has been interpreted in terms of a percolation model^[6], a model in which a transition from localized to extended states is important^[27] (as in the Anderson transition^[28] model), and a model based on a hopping mechanism of excitation transfer^[29].

Disordered solids in which both the transition energy and the

separation changes over a wide range have a number of properties not possessed by crystalline solids. First, the excitation energies of the different molecules in the disordered solid have a larger spread in excitation energy than in crystalline solids, resulting in a larger inhomogeneous linewidth for the former (100 cm^{-1} as compared to 1 cm^{-1} at 4.2 K). Second, in disordered solids, the distance between molecules that can exchange excitation energy is not constant, leading to a diffusion coefficient which changes in time^[30] after a pulsed excitation of the donor in the system. Third, using lasers, a set of molecules or ions within the inhomogeneous profile can be excited, thus acting as the donors. Some of the species of the same chemical remaining unexcited can act as the acceptors. If $kT > \Delta v_{inh}$, then all the unexcited species are indeed potential acceptors and the energy transfer process occurs to species of higher or lower frequency than the donor by phonon assisted processes^[31], e.g. between Eu^{3+} ions in phosphate glasses^[2,3]. If, however, $kT \ll \Delta v_{inh}$, only those species with transition frequencies equal or lower than those excited with the laser are potential acceptors, e.g. the transfer in ODS like BCN^[8-10] at 4.2 K. In these systems, the concentration of the potential acceptors can be changed continuously by simply changing the wavelength of a tunable laser used for excitation. Since the different energy transfer mechanisms may be of different dimensionality and are expected to be most effective at different ranges of donor-acceptor separation, i.e. at different time scales after the donor excitation, a switch in the excitation transfer mechanism from a shorter range and less isotropic interaction to a long range and more isotropic interaction

might be observed by analyzing the temporal dependence of an excited donor population at a certain acceptor concentration^[32], e.g. by adjusting the laser excitation wavelength at low temperatures. Such a behavior is not expected for crystalline materials.

The $T_1 - S_0$ transition of BCN at low temperatures has an inhomogeneous width on the order of 100 cm^{-1} . This linewidth is about two orders of magnitude larger than the linewidth observed for the corresponding transition in 1,4-dichloronaphthalene (DCN) and 1,4-dibromonaphthalene (DBN), suggesting that the width in BCN is due to the static orientational disorder in the halogen positions in the crystal^[12]. Comparative studies of the crystal structures^[33] and Raman spectra^[34] of this 1,4-dihalonaphthalene series show that the one-dimensional stacking feature and intermolecular interactions in BCN are similar to DBN for which one dimensional exchange-type triplet excitons have been observed^[35].

Recent results on the time resolved phosphorescence line narrowing (TRPLN) studies at 4.2 K ($kT \ll \Delta v_{inh}$) have shown^[8] that following pulsed narrowband excitation on the low energy side of the absorption profile that the line narrowed component (donor) decays with time while the emission from lower energy sites emerges uniformly. This is interpreted in terms of a unidirectional high to low energy transfer. The increase in the donor decay rate with increasing donor site energy is interpreted as arising from the increase in the mole fraction of lower energy acceptor sites as one moves to higher energies within the inhomogeneous profile.

In this paper, we present the temporal behavior of the

phosphorescence emission intensity of laser excited triplet energy donors in BCN at 4.2 K. From the analysis of the donor emission decay, the coupling mechanism can be inferred. This analysis is carried out as a function of the acceptor concentration (i.e. the excitation laser wavelength). The aim of these studies is to look for possible switching of the energy transfer mechanism in a disordered solid like BCN as the donor-acceptor separation (i.e. acceptor concentration) is changed. The results suggest that a possible switching from a one-dimensional exchange to a three-dimensional electric dipole-dipole mechanism takes place as the acceptor concentration is reduced below ten mole percent. At still larger donor-acceptor separation, none of the coupling mechanisms can compete with radiative processes, leading to excitation trapping. Based on this simple idea, a phenomenological description of the trapping process in these disordered solids is given which is found to account for the observed trapped emission in BCN and to give energy transfer parameters which are in reasonable agreement with the results obtained from the decay analysis of the temporal behavior discussed above. Preliminary reports of this work have recently been communicated^[9,10].

EXPERIMENTAL

The BCN was synthesized from 1-amino,4-chloronaphthalene by means of a procedure described elsewhere^[12]. The material was extensively zone refined. Crystals were grown from the melt in a Bridgmann furnace. The 4.2 K measurements were carried out with the sample immersed in liquid helium.

Spectra were recorded using a 1-M Jarrell-Ash monochromator with a

2 cm^{-1} resolution used throughout. Steady state phosphorescence spectra were obtained by excitation with the 3300 Å region of a 100 W mercury-xenon lamp. Absorption spectra were obtained with a 80 W quartz-halogen lamp. Signal was averaged with a PAR Model 162 boxcar averager, recorded on a Tracor-Northern NS-570A multichannel digitizer, and analyzed on a PDP-11/45 computer.

For time resolved measurements, a Quanta-Ray DCR-1 Nd:YAG pumped pulsed dye laser at a repetition rate of 10 Hz with a spectral width of 0.3 cm^{-1} and a pulse width of 6 nsec was used as the $T_1 - S_0$ excitation source. Time resolved spectra of the $T_1 - S_0$ phosphorescence of the 0,0-321 cm^{-1} band in the wavelength domain were recorded with the PAR boxcar averager. The temporal dependence of the donor phosphorescence was performed by carefully tuning the monochromator to the donor 0,0-321 cm^{-1} band so as to follow the donor intensity. Spectra were recorded with a Biomation 805 waveform digitizer, averaged with a homebuilt signal averaging computer, and analyzed on a PDP-11/45 computer. A special gated phototube was used in order to reject scattered laser light. Due to interference from switching the the focus electrode, the first 10 μsec of signal following the laser pulse was rejected. In order to estimate I_0 , the intensity at time $t=0$, I_0 was determined by extrapolating a $\log(I)$ vs. $\log(t)$ fit to the first 10 to 50 μsec of signal to $t=0$.

ABSORPTION and EMISSION SPECTRA of BCN

The broad features observed in the $T_1 - S_0$ absorption spectrum of BCN indicate that the singlet-triplet absorption in this system is inhomogeneously broadened. The nature of the inhomogeneous broadening

most likely arises from the static orientational disorder in the bromine and chlorine positions in the crystal. The orientational disorder leads to an inhomogeneous distribution of the site energy due to the disorder in the static crystal shift from the gaseous excitation energy. The absorption profile of the 0,0 band of the singlet-triplet transition of neat BCN at 4.2 K is shown in fig. 1. The general characteristics are in agreement with the spectrum reported in the literature^[12]. Shown in fig. 1 is a fit of the absorption profile to a Gaussian with a 32 cm^{-1} width (hwhm), suggesting an inhomogeneous type of broadening. A temperature dependent study of the absorption lineshape for BCN has shown that the homogeneous broadening due to interactions with phonons is much smaller than that due to the disorder^[12]. The broad, structureless, and nearly Gaussian absorption profile lend support to the interpretation that the inhomogeneous profile is determined by the static structural disorder.

The phosphorescence profile of the 0,0 band of the $T_1 - S_0$ transition of neat BCN is also shown in fig. 1, which agrees with that previously reported^[12]. The phosphorescence profile is observed to be narrower than the absorption profile and to originate from the low energy sites observed in absorption. These results indicate that at 4.2 K a rapid phonon assisted energy cascade from high to low energy sites occurs in neat BCN at 4.2 K. At temperatures where $kT \ll$ inhomogeneous width, energy transfer from low to high energy sites will be negligible since energy transfer from low to high energy sites requires the population of phonons which will be small in this temperature regime. We will return to the origin of the

phosphorescence profile after describing the results of the time resolved phosphorescence line narrowing (TRPLN) studies in this system.

DYNAMICS of SPECTRAL DIFFUSION in BCN

The results of the TRPLN studies reported in ref. 8 show that spectral diffusion of the $T_1 - S_0$ transition energy occurs in BCN, where the band shape of the first vibronic band was monitored as a function of delay time. The results show that the line narrowed component decreases in intensity preserving its width, while phosphorescence from the lower energy acceptors increases in intensity. The acceptor phosphorescence is observed to increase uniformly in time and at long times resembles the steady state phosphorescence of the 0,0-321 cm^{-1} band.

The results of the dependence of the rate of spectral diffusion on the donor site excitation energy reported in ref. 8 show that the energy transfer rate is strongly dependent on the donor excitation energy. Excitation at lower energies within the absorption profile result in phosphorescence mainly from the initially excited sites. With excitation at higher energies within the absorption profile the relative donor to lower energy acceptor phosphorescence decreases uniformly. For excitation at 4937 Å only the acceptor emission is observed on the time scale used. Excitation at higher energies within the inhomogeneous profile results in emission only from the lower energy sites. The phosphorescence from the low energy acceptors following pulsed excitation within the 0,0 absorption profile at energies higher than 4937 Å is similar in both width and position to the phosphorescence profile observed with steady state broadband

excitation of the $S_1 - S_0$ transition. These results show that the energy cascades down to the same energetic distribution of sites regardless of the initially excited site energy for energies higher than the phosphorescence profile.

The TRPLN results confirm that the absorption profile is inhomogeneously broadened and that a one way energy transfer from high to low energy sites occurs in this system. In the BCN system at 4.2 K, $kT \sim 3\text{cm}^{-1}$ while the inhomogeneous width is 64cm^{-1} (fwhm). At this temperature, transfer from low energy sites to higher energy sites by the absorption of one phonon is negligible since this process requires the population of phonons of energy $\Delta E_{12} \gg kT$, where ΔE_{12} is the energy mismatch between the donor and acceptor sites, which will be very small. For the same reason, the higher order Raman and Orbach type phonon assisted processes^[31] for transfer from low to high energy sites will also be unimportant at this temperature.

The time development of the low energy acceptor phosphorescence reported in ref. 8 shows that the initially excited line narrowed component decreases in time preserving its width while the low energy acceptor phosphorescence emerges uniformly resembling the steady state phosphorescence profile at all times. The acceptor phosphorescence does not simply reflect the energetic distribution of all of the lower energy acceptors which is given by the tail of the Gaussian for $E < E_1$, where E_1 is the energy of the initially excited donors. For symmetric energy transfer, where transfer to higher or lower energy sites occurs with a similar probability, the details of the emergence of the acceptor profile and the wavelength dependence of the energy transfer

rate can be used to determine the dependence of the energy transfer rate on the donor-acceptor energy mismatch^[25,31]. The interpretation of the energy mismatch dependence when energy transfer is observed to take place only to lower energy acceptor sites is complicated by the increase in the density of lower energy acceptors as the energy of the donor is increased. This could explain the increase in the energy transfer rate with increasing donor site energy. The analysis of the temporal development of the low energy acceptor phosphorescence is thus complicated by spectral diffusion within the acceptor system. For an initial transfer step from the initially excited donor at energy E_1 to an acceptor at energy E_2 where ΔE_{12} is small on the scale of the average donor-acceptor energy mismatch, the time scale of a second transfer step from E_2 to a still lower energy acceptor will be comparable to the initial transfer time from E_1 to E_2 . The occurrence of multiple transfer steps for a single excitation will prevent the observation of phosphorescence from the full acceptor density at higher acceptor energies. The emergence of the phosphorescence from the full spectrum of lower energy acceptors resembling the steady state phosphorescence profile regardless of the initial excitation energy indicates that the energy transfer process is only weakly dependent on the energy mismatch. The increase in the energy transfer rate with increasing donor excitation energy is then predominantly due to the increase in the density of acceptors. We now turn to the temporal dependence of the donor intensity and assume that the acceptor concentration can be described by the mole fraction of sites with energies equal to or less than the initial donor excitation energy.

TEMPORAL BEHAVIOR of the DONOR EXCITATION PROBABILITY

The inhomogeneous broadening of the $T_1 - S_0$ transition energy in BCN is assumed to be microscopic in nature with a random spatial distribution of transition energies. A high degree of correlation in site energies would most likely result in a distortion of the low energy acceptor phosphorescence profile with different excitation wavelengths due to preferential energy transfer to a particular type of acceptor. The uniformity of the acceptor phosphorescence with time and donor excitation wavelength suggest that the site energies are to a good degree uncorellated, at least on the low energy tail of the absorption profile where all of our measurements have been made. The random nature of the site energies at the low energy side of the absorption profile results in a distribution of the distances between donor and lower energy acceptors. For a single donor acceptor pair the energy transfer rate $W(R)$, where R is the position of the acceptor, can be written as [36,37]

$$W(R) = \frac{1}{\tau} \exp[\gamma(d-R)] \quad (1)$$

for isotropic exchange coupling, and

$$W(R) = \frac{1}{\tau} (d/R)^s \quad (2)$$

for isotropic multipolar interactions. Equ. 1 and 2 are expressed in terms of d , the nearest neighbor distance, and τ , the transfer time from a donor to an acceptor at a distance d . In equ. 1, γ is a measure of the dependence of the transfer rate on distance for exchange coupling. The exponent s in equ. 2 is 6, 8, 10 for electrostatic dipole-dipole, dipole-quadrupole, or quadrupole-quadrupole interactions respectively.

In order to describe the time dependence of the donor excitation probability, $P(t)$, in a macroscopic system, a statistical averaging of the distances R is necessary. The distance averaging was first treated by Inokuti and Hirayama^[22] for exchange and multipolar interactions in three dimensions and later generalized to all dimensions for both exchange^[24] and multipolar^[23] interactions. The time dependence of the donor excitation probability, after correcting for the first order radiative decay, for exchange coupling can be described by^[24]

$$\ln[P(t)] = -aV_{\Delta} (\gamma_d)^{-\Delta} c g_{\Delta}\left(\frac{t}{\tau} \gamma_d\right) \quad (3)$$

where V_{Δ} is the volume of a unit sphere in a space of Δ dimensions,

a is a constant ~ 1 whose exact value depends on the lattice geometry, and c is the acceptor concentration. The function $g_{\Delta}\left(\frac{t}{\tau} \gamma_d\right)$ is given by^[24]

$$g_1\left(\frac{t}{\tau} \gamma_d\right) = \ln\left[\frac{t}{\tau} \gamma_d\right] + 0.57722 \quad (4a)$$

$$g_2\left(\frac{t}{\tau} \gamma_d\right) = \ln^2\left[\frac{t}{\tau} \gamma_d\right] + 1.15443 \ln\left[\frac{t}{\tau} \gamma_d\right] + 1.97811 \quad (4b)$$

$$g_3\left(\frac{t}{\tau} \gamma_d\right) = \ln^3\left[\frac{t}{\tau} \gamma_d\right] + 1.73165 \ln^2\left[\frac{t}{\tau} \gamma_d\right] + 5.93434 \ln\left[\frac{t}{\tau} \gamma_d\right] + 5.44487 \quad (4c)$$

For multipolar interactions, the time dependence of the donor excitation probability, after correcting for the first order radiative decay, can be described by^[23]

$$\ln[P(t)] = -V_{\Delta} \Gamma\left(1 - \frac{\Delta}{s}\right) c (t/\tau)^{\Delta/s}, \quad (5)$$

where $\Gamma(1-s)$ is the gamma function. The above results were obtained for low acceptor concentrations and neglecting back transfer from acceptor to donor.

It is generally accepted that triplet-triplet energy transfer in organic molecular crystals is of the exchange type. Though the nature of the exchange interaction is of short range, even trap to trap

migration of triplet excitations over an order of 10 intervening host molecules in mixed organic crystals has been interpreted in terms of exchange or superexchange^[38]. In a study of the exciton dynamics in DBN^[35], it was found that the exciton could well be described by a one dimensional behavior along the DBN stack with a nearest neighbor exchange coupling β of 7.4 cm^{-1} , where $\tau = h/\beta$. The one dimensional behavior was attributed to the strong $p\pi$ orbital overlap between nearest neighbors in a direction almost perpendicular to the molecular plane. In a comparative study of the crystal structures of the 1,4-dihalonaphthalenes it was found that although DCN and BCN crystallize in a somewhat different structure ($P2_1/c, Z=4$) than DBN ($P2_1/c, Z=8$) both structures show a very similar stacking feature suggesting that the BCN structure should also show a one dimensional intermolecular interaction^[33]. The study of the Raman spectra in the neat and mixed crystals has suggested that the intermolecular interactions in the 1,4-dihalonaphthalenes are similar^[34].

Because of the similarities of the interactions in the BCN crystal to those in the DBN crystal, where one dimensional exchange-type excitons are observed, we will first examine the temporal dependence of the donor phosphorescence intensity in terms of one dimensional exchange interactions in order to test if this dimensionality and type of interaction is preserved for the long range (greater than nearest neighbor at low acceptor concentrations), nonresonant energy transfer that results from the inhomogeneity of the $T_1 - S_0$ transition in BCN. The fit of the donor excitation probability after correcting for the first order radiative decay, $P(t)$, to the one dimensional exchange

mechanism using eqs. 3 and 4a for several excitation wavelengths on the low energy tail of the 0,0 band of the $T_1 - S_0$ transition of BCN is shown in fig. 2 where we plot $\log[P(t)]$ vs. $\log(t)$. The quantity $P(t) = I(t)\exp(t/\tau_0)$, where $I(t)$ is the phosphorescence intensity normalized to one at $t=0$ and τ_0 is the radiative lifetime in the absence of energy transfer. On this choice of scales, the decay should be linear for energy transfer to randomly distributed acceptors in one dimension by the exchange mechanism with a slope of $-c/\gamma d$. The fit to this mechanism and dimensionality at short times, although poor at longer wavelengths (lower acceptor concentrations), is very good at shorter wavelengths (4940 Å) where the acceptor concentration is higher.

We now discuss the acceptor concentration dependence of the slopes of the fit to the one dimensional exchange mechanism shown in fig. 2. We have previously described the acceptor concentration in the BCN system at 4.2 K as the mole fraction of BCN molecules whose $T_1 - S_0$ transition frequencies, ν , are $<$ the donor transition frequency, ν_{exc} . For a Gaussian distribution of site energies, the mole fraction of sites having transition frequencies $< \nu$, X_ν , is given by

$$X_\nu = \int^{-1} \left(\frac{\ln 2}{\pi} \right)^{1/2} \exp[-\ln 2 ((\nu' - \nu_{max})/\Gamma)^2] d\nu' \quad (6)$$

where Γ is the Gaussian width (hwhm) centered at ν_{max} . From fig. 1 we find $\Gamma = 32 \text{ cm}^{-1}$ and $\nu_{max} = 20284 \text{ cm}^{-1}$ for the 0,0 band of the $T_1 - S_0$ transition of BCN at 4.2 K. The magnitude of the slope of the 1-D exchange fit, $-m_{1-D,E}$ vs. X_ν is shown in fig. 3. The solid line is the graph of $-m_{1-D,E} = X_\nu/\gamma d$ where $\gamma d = 0.1$. Exchange interactions are usually of shorter range, i.e. $\gamma d \gg 1$, with $\gamma d = 5$ being typical for

many aromatic systems^[39]. For illustrative purposes, the expected concentration dependence of $-m_{1-D,E}$ for γ_d equal to 5 is also displayed in fig. 3. From the poor fit of the 1-D exchange mechanism we conclude that this mechanism is not the dominant energy transfer mechanism for the excitation energies used here. At these relatively low acceptor concentrations, superexchange, rather than the exchange mechanism may be expected to be dominant. For the superexchange mechanism the rate of energy transfer at a distance $(N+1)d$ is given by^[38]

$$W(R) = \frac{1}{\tau} \exp(N \ln(\beta/\Delta E)) \quad (7)$$

where ΔE is the separation between host and donor singlet-triplet transition energies and is $\gg \beta$. From the similarity of equs. 1 and 7 one can see that the form of the superexchange interaction is the same as the exchange interaction with $-\ln(\beta/\Delta E)$ equivalent to γ_d . Equ. 3 may then describe the donor excitation probability with $\gamma_d = -\ln(\beta/\Delta E)$. We define the host species in BCN as those molecules with transition frequencies $\nu > \nu_{exc}$. Taking the absorption maximum as an effective host energy level one obtains $\Delta E = 37$ to 70 cm^{-1} for the excitation energies used here. For $\beta \ll 37 \text{ cm}^{-1}$ the temporal decay of the donor excitation probability should be linear on a $\log[P(t)]$ vs. $\log(t)$ scale for the superexchange mechanism. The poor fit at the longer excitation wavelengths shown in fig. 2 indicate that the superexchange mechanism is also not important at low acceptor concentrations. For excitation at 4940 Å, the decay appears to fit the superexchange mechanism with $-m_{1-D,E} = 0.78$. Taking $-m_{1-D,E} = c/[-\ln(\beta/\Delta E)]$ with $c = 0.066$ from equ. (6) and $\Delta E = 41 \text{ cm}^{-1}$ for excitation at 4940 Å, one

obtains $\beta = 38 \text{ cm}^{-1}$ for BCN. This value is much greater than the 7.4 cm^{-1} value observed for β in the DBN crystal which should show a similar exchange coupling. It also yields a value for $\Delta E/\beta$ of about unity for which the description of the superexchange coupling in equ. 7 may not be entirely valid. In addition, the description of the superexchange coupling given in equ. 7 assumes a constant energy separation ΔE . In the BCN system, however, the individual host energy levels are not constant, with a spread of transition frequencies given by $\Delta \nu_{\text{inh}}$. The use of equ. 7 for the description of the superexchange coupling with an effective ΔE , and the subsequent analysis using equ. 3, may not be adequate for this system, where the disorder in host energy levels is comparable to ΔE . A theoretical examination of the superexchange mechanism for energy transfer in a disordered host is indeed needed.

We now consider the possibility that the energy transfer in the BCN system at the long wavelength region of the absorption band where the acceptor concentration is low may arise from more isotropic interactions. One dimensional exchange type interactions have been found to be unable to account for the temporal dependence of the donor excitation probability. At low acceptor concentrations, where energy transfer to acceptor sites at distances greater than the nearest neighbor distance is important, more isotropic interactions may dominate over a one dimensional interaction. We now examine the temporal dependence of the donor excitation probability in terms of the dipole-dipole interaction in three dimensions since this interaction is more isotropic and also has a slower distance dependence than the

exchange interaction in this crystal.

The fit of the $P(t)$ to the three dimensional dipolar interaction using equ. 5 for the same excitation wavelengths used in fig. 2 is shown in fig. 4 where we plot $\log[P(t)]$ vs. $t^{1/2}$. On this choice of scales the decay should be linear with a slope proportional to the acceptor concentration. At the longest wavelength (4947 Å) the decay is well described by the 3-D dipole-dipole form, while at shorter wavelengths deviations from the fit are observed at early times. At 4940 Å we were unable to fit any sizable portion of the decay to the dipolar form. These results suggest that at long excitation wavelengths (low acceptor concentration) and at long times that the dipolar interaction dominates the energy transfer in this system. At short times and short excitation wavelengths (corresponding to shorter donor-acceptor distances) other interactions become important and the decay curve deviates from the dipolar form. At shorter donor-acceptor distances the one-dimensional exchange or possibly three dimensional exchange interactions most likely become important also. For excitation at 4940 Å, which correspond to relatively high acceptor concentration, both exchange and dipolar interactions may be active, which could account for our inability to interpret the decay in terms of only one mechanism.

As further evidence of the dipolar nature of the decay, we show in fig. 5 the acceptor concentration dependence of $-m_{3D,D-D}$, where $m_{3D,D-D}$ is the slope of the fitted line in the $\log[P(t)]$ vs. $t^{1/2}$ plot. $m_{3D,D-D}$ shows the predicted linear dependence on concentration according to equ. 5. The solid line in fig. 5 is the best fit line

with $\tau_{3D,D-D} = 1.8 \mu\text{sec}^{-1/2}(c + 0.013)$. Although $\tau_{3D,D-D}$ does not extrapolate to zero at zero acceptor concentration, this may be due to either errors in our estimation of the acceptor concentration from the assumption of a Gaussian absorption profile (see fig. 1) or from contributions to the decay from exchange coupling. For $\tau_{3D,D-D} = 1.3 \mu\text{sec}^{-1/2}c$, one obtains from equ. 5 a value for the transfer time at the nearest neighbor distance for dipolar coupling = 17 μsec .

TRAP PHOSPHORESCENCE PROFILE of BCN at 4.2 K

In the previous sections we have described the spectral diffusion in the BCN system at 4.2 K in terms of a one way high to low energy transfer process in which the increasing mole fraction of lower energy acceptors as one goes to higher energies within the inhomogeneously broadened $T_1 - S_0$ absorption profile plays an important role. These features are manifested in the phosphorescence profile of the same transition which is narrower than the absorption profile and originates from the lower energy sites. In this section we develop a simple model for the phosphorescence profile in which the energy cascades down from higher to lower energy sites until sites are reached for which the transfer rate becomes slower than the radiative decay rate.

The decay of an energetically excited donor site in the presence of acceptors can occur by radiative and nonradiative unimolecular process or by the donor transferring its excitation nonradiatively to an acceptor. The radiative and nonradiative unimolecular processes are taken to be independent of the nature of the excited site and to occur with a rate of $1/\tau_0$, where τ_0 is the decay time in the absence of acceptors. In the presence of acceptors the donor may transfer its

energy nonradiatively through either multipolar or exchange type interactions where $W(R)$ is given in equs. 1, 2, and 7 for exchange, multipolar, and superexchange interactions, respectively. One can define an interaction radius, R' , as the donor-acceptor distance for which the energy transfer rate is equal to the unimolecular decay rate [37]. From equs. 1, 2, and 7 one finds

$$R_0 = R'/d = (\tau_0/\tau)^{1/s} \quad (8a)$$

$$R_0 = 1 + \frac{1}{\gamma d} \ln(\tau_0/\tau) \quad (8b)$$

$$R_0 = 1 + \frac{1}{-\ln(\beta/\Delta E)} \ln(\tau_0 \beta/h) \quad (8c)$$

for multipolar, exchange, and superexchange interactions, respectively, where R_0 is the interaction radius in units of the lattice spacing, d . The radiative quantum yield, $\Phi(R)$, for a donor with an acceptor at distance R is given by

$$\Phi(R) = \frac{\tau_0^{-1}}{\tau_0^{-1} + W(R)} \quad (9)$$

where τ_0 is the radiative decay rate. Using equs. 8a and 8b one can write the quantum yield in terms of R' as

$$\Phi(R) = [1 + (R'/R)^s]^{-1} \quad (10a)$$

$$\Phi(R) = [1 + \exp(\gamma d(R'/d - R/d))]^{-1} \quad (10b)$$

for multipolar and exchange interactions respectively. A form similar to 10b exists for the superexchange interaction. Eqs 10a and 10b yield sigmoid type curves with $\Phi(R) = 1/2$ at $R = R'$. We now approximate 10a and 10b with a step function where $\Phi(R) = 0$ if $R < R'$ and $\Phi(R) = 1$ if $R > R'$. An electronically excited molecule with no lower energy acceptors at a distance $R < R'$ is then assumed to emit

radiation while a molecule with a lower energy acceptor at $R < R'$ will transfer its excitation before emitting and will not be seen in emission. The number of sites (excluding the one occupied by the donor) within the interaction volume, n , is given by

$$n = 4/3\pi R_0^3 - 1 \quad (11a)$$

$$n = 2\pi R_0^2 - 1 \quad (11b)$$

$$n = 2R_0 - 1 \quad (11c)$$

for 3-D, 2-D, and 1-D interactions, respectively.

We now consider the steady state excitation of sites on the high energy side of the inhomogeneous profile where the probability of an acceptor site being in the interaction volume of the initially excited site is near unity. The initial excitation will thus transfer exothermally with unit probability. The exothermic energy transfer process continues until a site is reached for which no lower energy acceptors lie within the interaction volume. The excitation is thus trapped and will then radiate. Assuming that the initial excitation finds these trapping sites with equal probability, the emission profile will represent the energetic distribution of sites for which no lower energy acceptors lie within the interaction volume. The distribution of trapping sites, $I(v)$, can be obtained from calculating as a function of v , the product of the probability that a site at energy v has no lower energy acceptors within the interaction volume, $Pr(v)$, and the relative number of sites at energy v , $N(v)$, i.e.

$$I(v) = \text{Const.} Pr(v) N(v) \quad (12)$$

The probability, $Pr(v)$, that an energetically excited site has no lower energy acceptors within the interaction volume given by n is $(1 -$

$X_v)^n$. For an inhomogeneously broadened single component (i.e. neat) crystal with a Gaussian absorption profile, the corresponding emission profile, $I(v)$, is given by

$$I(v) = \text{Const.}(1 - X_v)^n \exp(-\ln 2((v - v_{\max})/\Gamma)^2), \quad (13)$$

where X_v is given by equ. 6. For an optically active guest species in a spectrally inert host lattice where the guest species occupy the host lattice with probability p (given by the overall mole fraction of the guest), equ. 12 still holds with $X_v = X_v'p$, where X_v' is determined from the guest absorption profile using equ. 6.

The emission lineshape for several values of n in the range of 10 to 10,000 sites for a single component disordered crystal are displayed in fig. 6, along with the Gaussian absorption profile. Fig. 6 illustrates that as the interaction volume gets larger, the emission profile is shifted further to lower energy and the emission linewidth narrows. These results can be understood with the physical model used here. For a particular energetically excited site, the probability of finding a lower energy acceptor site within the interaction volume grows with the interaction volume. The energetic distribution of trapped sites is thus shifted to lower energy where the concentration of possible lower energy acceptors is smaller. The shift in the emission maximum from the absorption maximum and the emission linewidth vs. the interaction volume are plotted in figs. 7 and 8, respectively. From the absorption and emission spectra of a system, one can find n from the energy difference of the absorption and emission maxima using fig. 7. Similarly one can also determine n using the emission linewidth and fig. 8. Knowing n , one can infer the

microscopic energy transfer parameters in eqs. 1, 2, or 7 from eqs. 8 assuming a particular coupling mechanism and dimensionality.

The phosphorescence profile of the 0,0 band of BCN at 4.2 K along with the calculated emission spectrum using equ. 13 with $n = 365$ sites is shown in fig. 1, where the calculated and observed spectra are found to be in good agreement. We now discuss this interaction volume in terms of the different energy transfer mechanisms which might be expected to be important in BCN. The 365 sites contained in the interaction volume would yield an interaction radius, R_0 , of 182 for a one dimensional interaction. Using $\beta = 7.4 \text{ cm}^{-1}$, $\tau_0 = 20 \text{ msec}$ for BCN one obtains from equ. 8b a value for direct exchange of $\gamma_d = 0.1$. Exchange interactions are usually of shorter range, i.e. $\gamma_d \gg 1$, with $\gamma_d = 5$ being typical for many aromatic systems^[39]. For superexchange, one can estimate ΔE in this system as the energy separation between absorption and emission maxima. Using $\Delta E = 76 \text{ cm}^{-1}$ one finds $\beta = 66 \text{ cm}^{-1}$ for the 1-D superexchange mechanism. This value of β is about an order of magnitude larger than the value determined for DBN. Considering three dimensional interactions with $n = 365$ sites, one obtains $R_0 = 4.5$. For direct exchange in three dimensions, using $\beta = 7.4 \text{ cm}^{-1}$ as an upper limit for the isotropic exchange interaction, one obtains $\gamma_d < 7$ using equ. 8b. For superexchange with $\Delta E = 76 \text{ cm}^{-1}$ one obtains an isotropic $\beta = 0.6 \text{ cm}^{-1}$ from equ. 8c. For dipole-dipole coupling in three dimensions one obtains from equ. 8a a value for the nearest neighbor transfer time $\tau = 2.6 \text{ } \mu\text{sec}$. The results of this analysis of the phosphorescence profile provide further support to the conclusion that the energy transfer is three dimensional for

excitations on the low energy side of the absorption profile. At higher excitation energies where nearest neighbor transfer is important, the energy transfer may be one dimensional. The fit of the emission profile to equ. 13 gives the interaction volume for the interaction with the largest range. An interaction with a smaller range, even with a stronger coupling within that range, would be unimportant in determining the emission profile.

Acknowledgments: The authors would like to thank Prof. P. Prasad for our initial collaboration on this work and for supplying us with the sample. MAE would like to thank Drs. A. Blumen, S. Fischer, and E. Knapp of the theoretical group of the Technical University of Munich for many helpful discussions. MAE would like to thank the Alexander von Humbolt foundation for a Senior Humbolt Award spent in Munich (Feb - August 1982). The financial support of the Office of Naval Research is greatly appreciated.

REFERENCES

1. N. Motegi and S. Shionoya, J. Lumin. 8, 1 (1973).
2. M. A. El Sayed, A. Campion, and P. Avouris, J. Mol. Struct. 46, 355 (1978).
3. P. Avouris, A. Campion, and M. A. El Sayed, Chem. Phys. Lett. 50, 9 (1977).
4. S. Chu, H. M. Gibbs, S. L. McCall, and A. Passner, Phys. Rev. Lett. 45, 1715 (1980).
5. J. R. Morgan and M. A. El Sayed, J. Phys. Chem. 85, 3566 (1981).
6. R. Kopelman, E. Monberg, and F. W. Ochs, Chem Phys. 19, 413 (1977).
7. D. D. Smith, R. D. Mead, and A. H. Zewail, Chem. Phys. Lett. 50, 358 (1977).
8. P. N. Prasad, J. R. Morgan, and M. A. El Sayed, J. Phys. Chem. 85, 3569 (1981).
9. J. R. Morgan and M. A. El Sayed, J. Phys. Chem., in press.
10. J. R. Morgan and M. A. El Sayed, J. Phys. Chem., in press.
11. A. I. Kitaigorodsky, 'Molecular Crystals and Molecules', Academic Press, New York, 1973.
12. J. C. Bellows and P. N. Prasad, J. Phys. Chem. 86, 328 (1982).
13. P. M. Selzer, D. L. Huber, D. S. Hamilton, W. M. Yen, and M. J. Weber, Phys. Rev. Lett. 36, 813, (1976).
14. J. Hegarty and W. M. Yen, Phys. Rev. Lett. 43, 1126 (1979).
15. T. L. Reinecke, Solid State Commun. 32, 1103 (1979).
16. S. K. Lyo and R. Orbach, Phys. Rev. B22, 4223 (1980).
17. S. K. Lyo, Phys. Rev. Lett. 48, 668 (1982).

18. P. Reineker and H. Morawitz, *Chem. Phys. Lett.* 86, 359 (1982).
19. P. W. Anderson, B. I. Halperin, and C. M. Varma, *Philos. Mag.* 25, 1 (1972).
20. W. A. Phillips, *J. Low Temp. Phys.* 7, 351 (1972).
21. J. R. Morgan, E. P. Chock, W. D. Hopewell, M. A. El Sayed, and R. Orbach, *J. Phys. Chem.* 85, 747 (1981).
22. M. Inokuti and F. Hirayama, *J. Chem. Phys.* 43, 1978 (1965).
23. A. Blumen and J. Manz, *J. Chem. Phys.* 71, 4694 (1979).
24. A. Blumen, *J. Chem. Phys.* 72, 2632 (1980).
25. P. M. Selzer in 'Topics in Applied Physics', vol.49, *Laser Spectroscopy of Solids*, ed. W. M. Yen and P. M. Selzer (Springer, Berlin, 1982), chap. 4, and ref. therein.
26. D. P. Craig and S. H. Walmsley, 'Excitons in Molecular Crystals', W. A. Benjamin, Amsterdam, 1968.
27. J. Klafter and J. Jortner, *Chem. Phys. Lett.* 49, 410 (1977).
28. P. W. Anderson, *Phys. Rev.* 109, 1492 (1958).
29. A. Blumen and R. Silbey, *J. Chem. Phys.* 70, 3707 (1979).
30. S. W. Haan and R. Zwanzig, *J. Chem. Phys.* 68, 1879 (1978).
31. T. Holstein, S. K. Lyo, and R. Orbach, *Phys. Rev. Lett.* 36, 891 (1976).
32. J. Klafter and R. Silbey, *J. Chem. Phys.* 72, 849 (1980).
33. J. C. Bellows, E. D. Stevens, and P. N. Prasad, *Acta Crystallogr.* B34, 3256 (1978).
34. J. C. Bellows and P. N. Prasad, *J. Chem. Phys.* 67, 5802 (1979).
35. R. M. Hochstrasser and J. D. Whiteman, *J. Chem. Phys.* 56, 5945 (1972).

36. T. Forster, Z. Naturforsch. Teil A 4, 321 (1949).
37. D. L. Dexter, J. Chem. Phys. 21, 836 (1953).
38. G. G. Niemann and G. W. Robinson, J. Chem. Phys. 37, 2150
(1962).
39. A. Blumen and R. Silbey, J. Chem. Phys. 70, 3707 (1979).

FIGURE CAPTIONS

Fig. 1 The emission and absorption spectra of the $T_1 - S_0$ transition of 1-bromo,4-chloronaphthalene (BCN) at 4.2 K. The observed absorption profile of the zero phonon line of the 0,0 band is fitted to a Gaussian centered at 20284 cm^{-1} with $\Gamma = 32 \text{ cm}^{-1}$ (solid line). The observed narrowed emission profile centered at 20208 cm^{-1} along with the calculated emission lineshape (solid line) using eq. 12 with $n = 365$ sites.

Fig. 2 The fit of the early portion of the decay of the triplet excitation due to triplet-triplet energy transfer to an exchange mechanism for different excitation wavelengths (4947 Å, 4943 Å, 4942 Å, and 4940 Å from top to bottom, respectively) within the 0,0 band of the $T_1 - S_0$ transition in 1-bromo,4-chloronaphthalene at 4.2 K. The range of the fit increases as the excitation wavelength decreases, i. e., as the acceptor concentration increases.

Fig. 3 The magnitude of the slope of the 1-D exchange fit ($-m_{1-D,E}$) to the early portion of the decay of the triplet excitation shown in fig. 2 vs. the mole fraction of lower energy acceptors (X_V) determined from eqn. 6 for BCN at 4.2 K. The solid line is the graph of $-m_{1-D,E} = X_V/\gamma d$ where $\gamma d = 0.1$. The dashed line is for $\gamma d = 5$, a value typical for many aromatic systems^[39].

Fig. 4 The fit of the long time portion of the decay of the triplet excitation of the 0,0 band of the $T_1 - S_0$ transition of 1-bromo,4-chloronaphthalene at 4.2 K due to triplet-triplet energy transfer to a three dimensional dipolar mechanism for the excitation wavelengths given in fig. 2. The range of the fit is better at longer

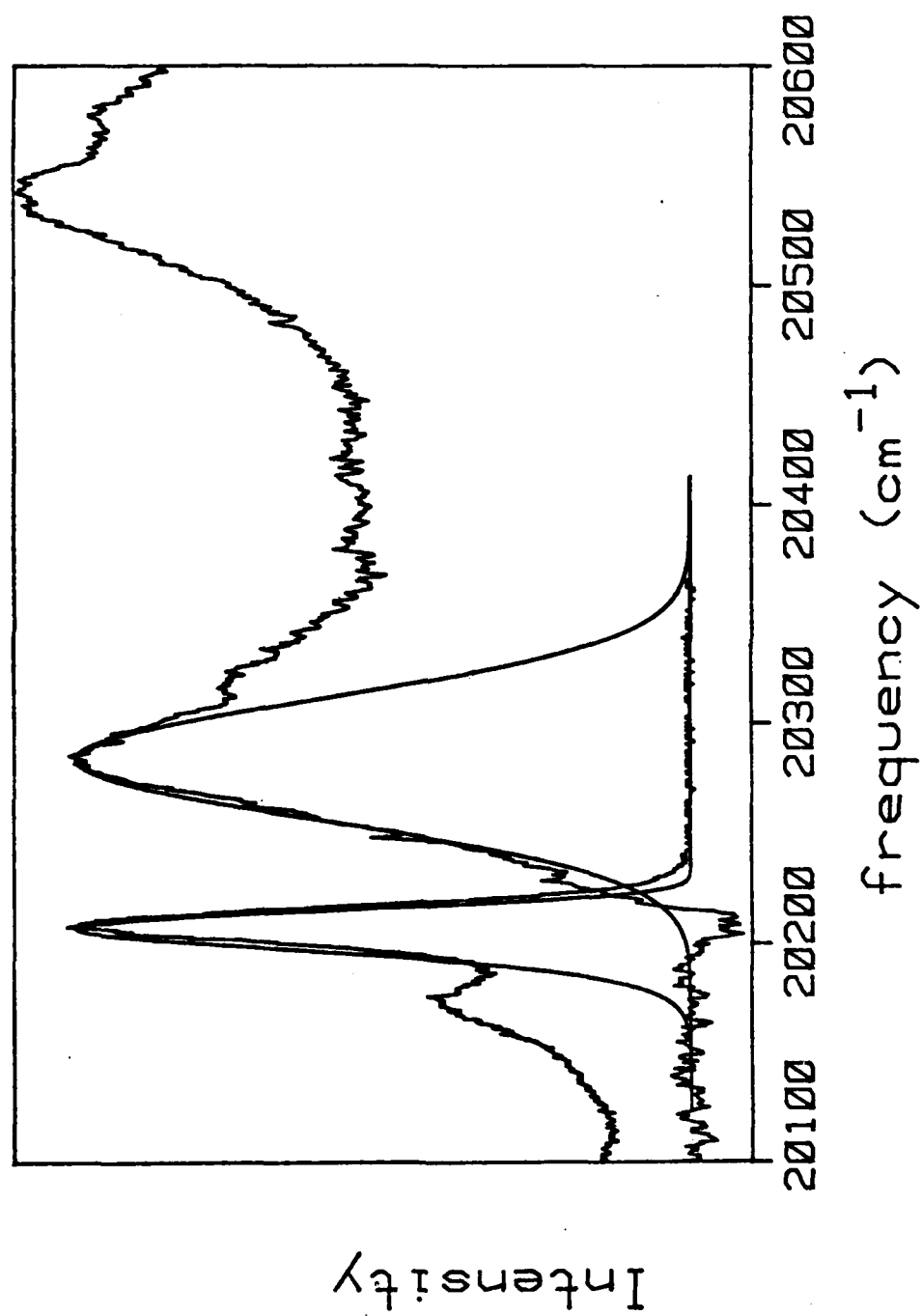
excitation wavelengths, i. e., at low acceptor concentrations.

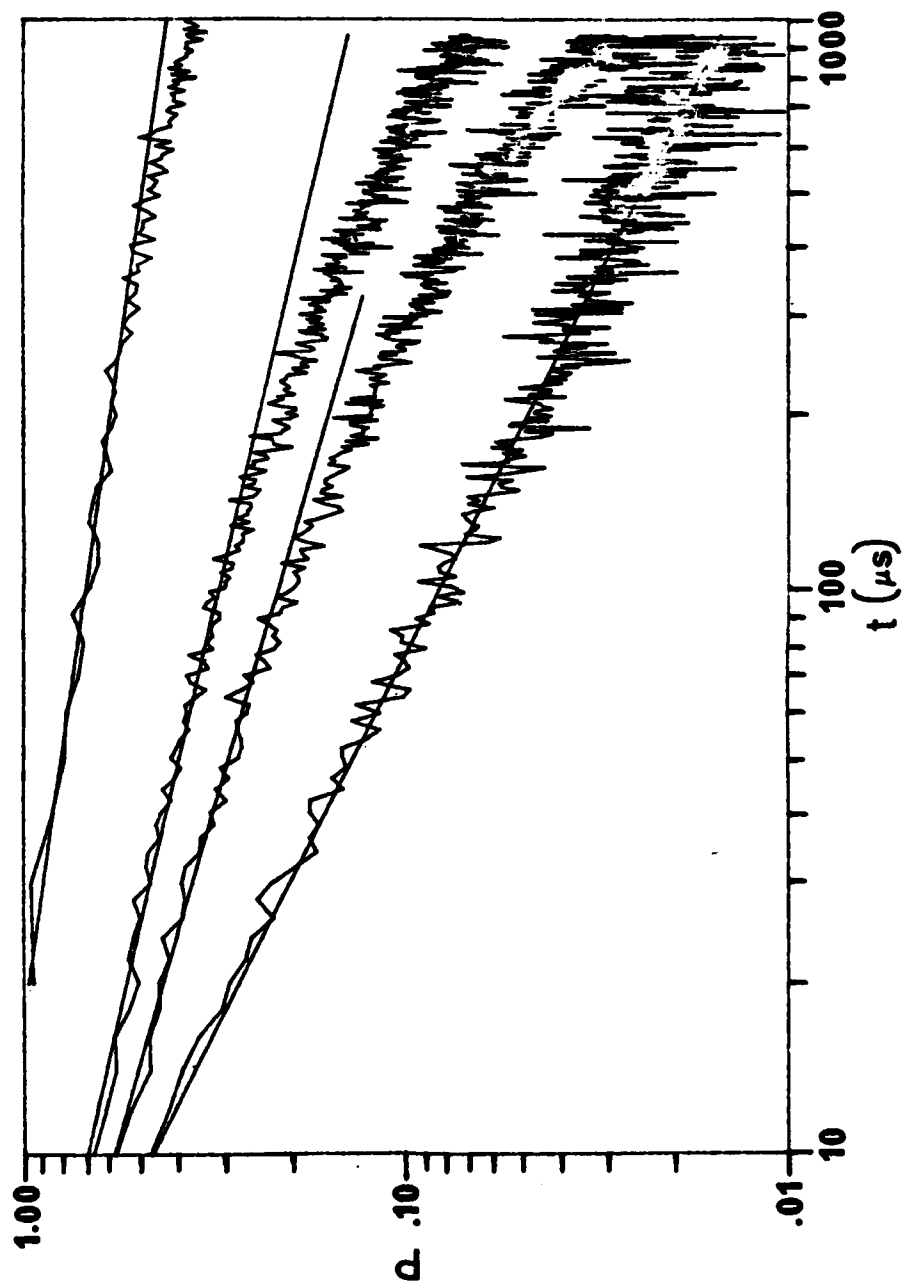
Fig. 5 The magnitude of the slope of the 3-D dipole-dipole fit ($m_{3-D,DD}$) to the long time portion of the triplet excitation shown in fig. 4 vs. the mole fraction of lower energy acceptors (X_v) for BCN at 4.2 K. $m_{3-D,DD}$ shows the predicted linear dependence on acceptor concentration for dipole-dipole coupling.

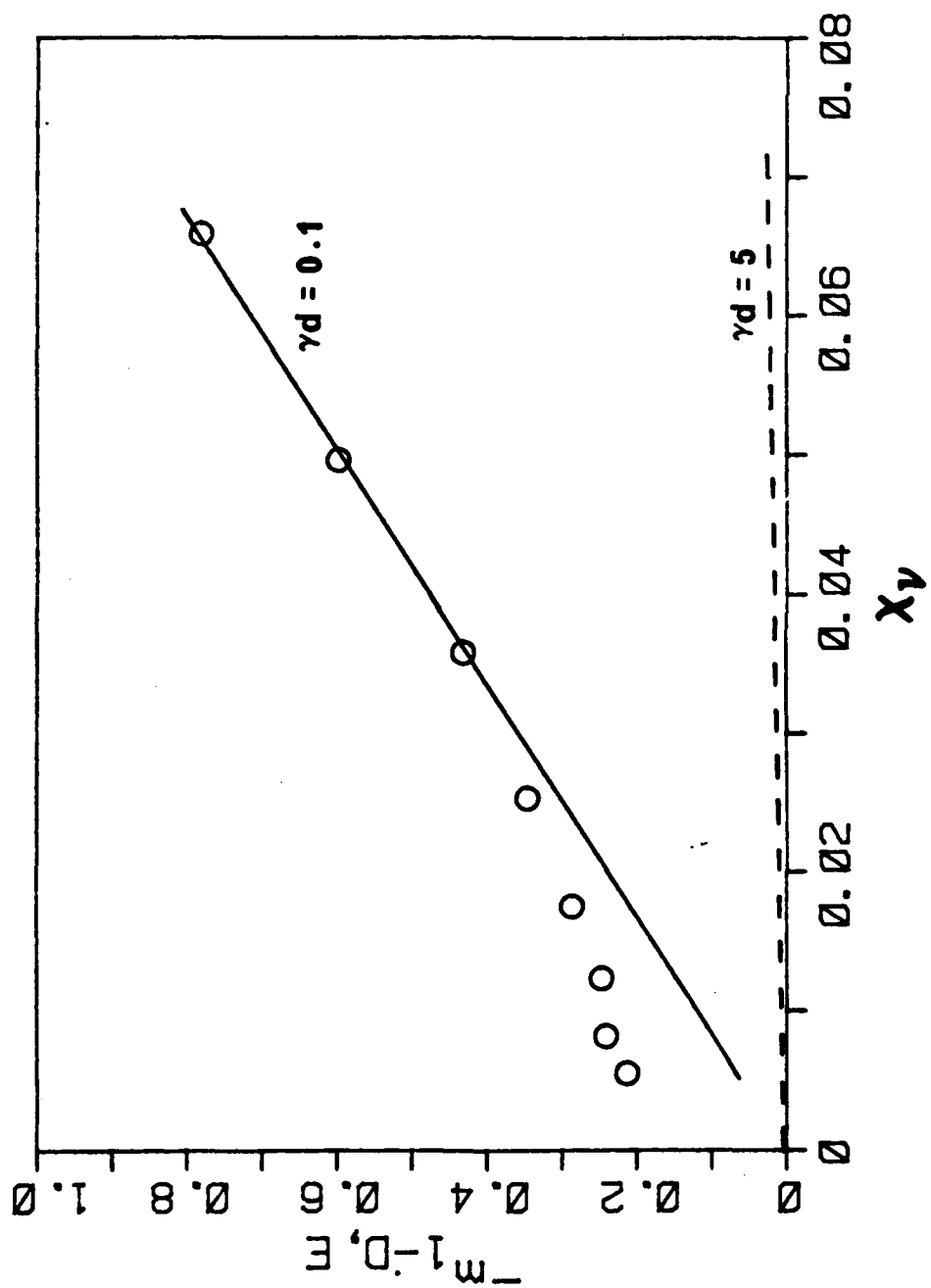
Fig. 6 The emission profile $I(v)$ for a Gaussian absorption profile in a single component crystal with an energy transfer interaction volume of n sites. Plotted from right to left are the Gaussian absorption profile and the emission profiles for $n = 10^1$, 10^2 , 10^3 , and 10^4 sites respectively. The emission profile is found to shift to lower energy and to narrow in width with increasing n .

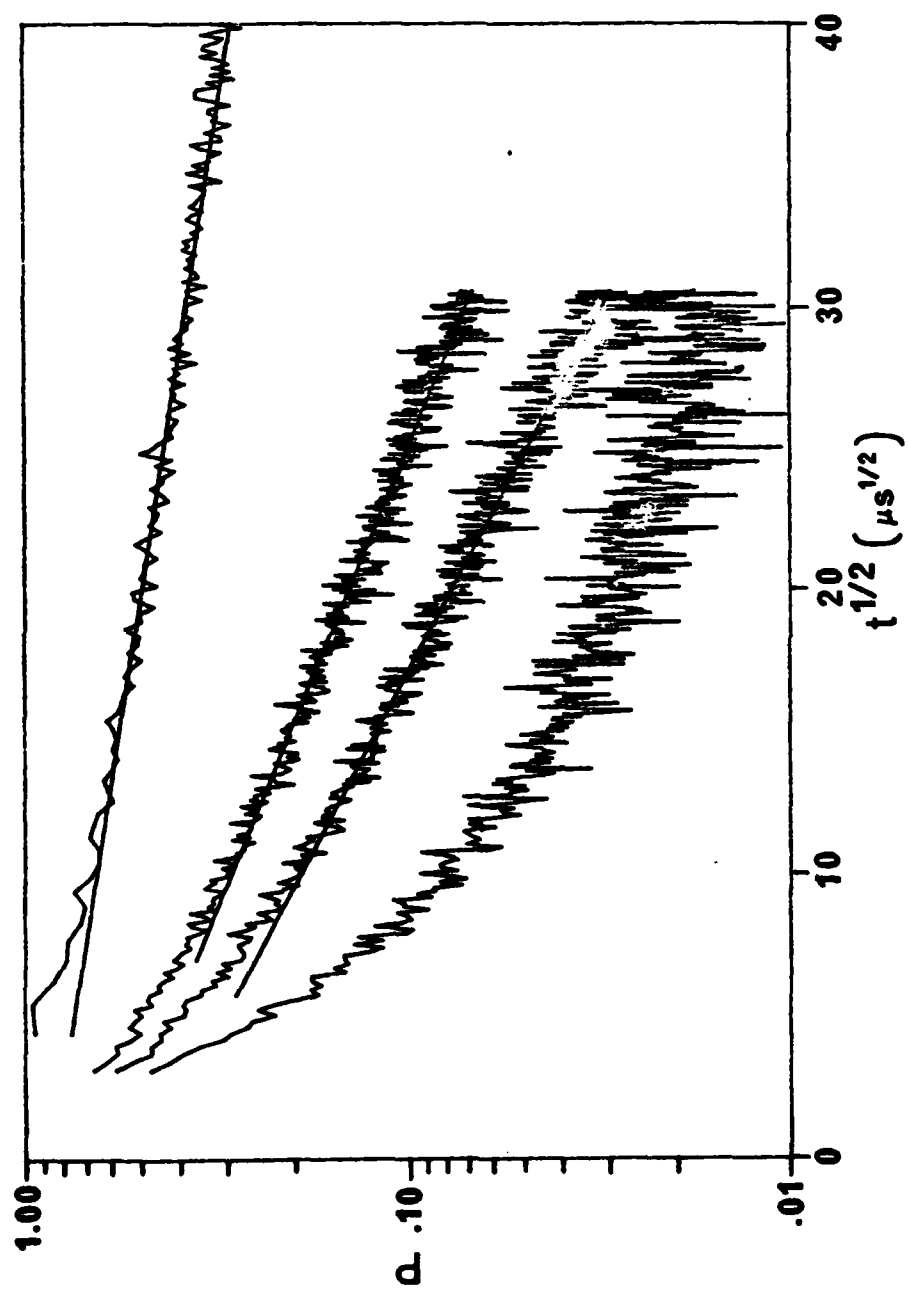
Fig. 7 The shift in the guest emission maximum from the absorption maximum normalized by the Gaussian absorption width Γ (hwhm) vs. the interaction volume n . From bottom to top, these curves are for guest mole fractions $p = 1.0$, 0.5 , 0.2 and 0.1 respectively.

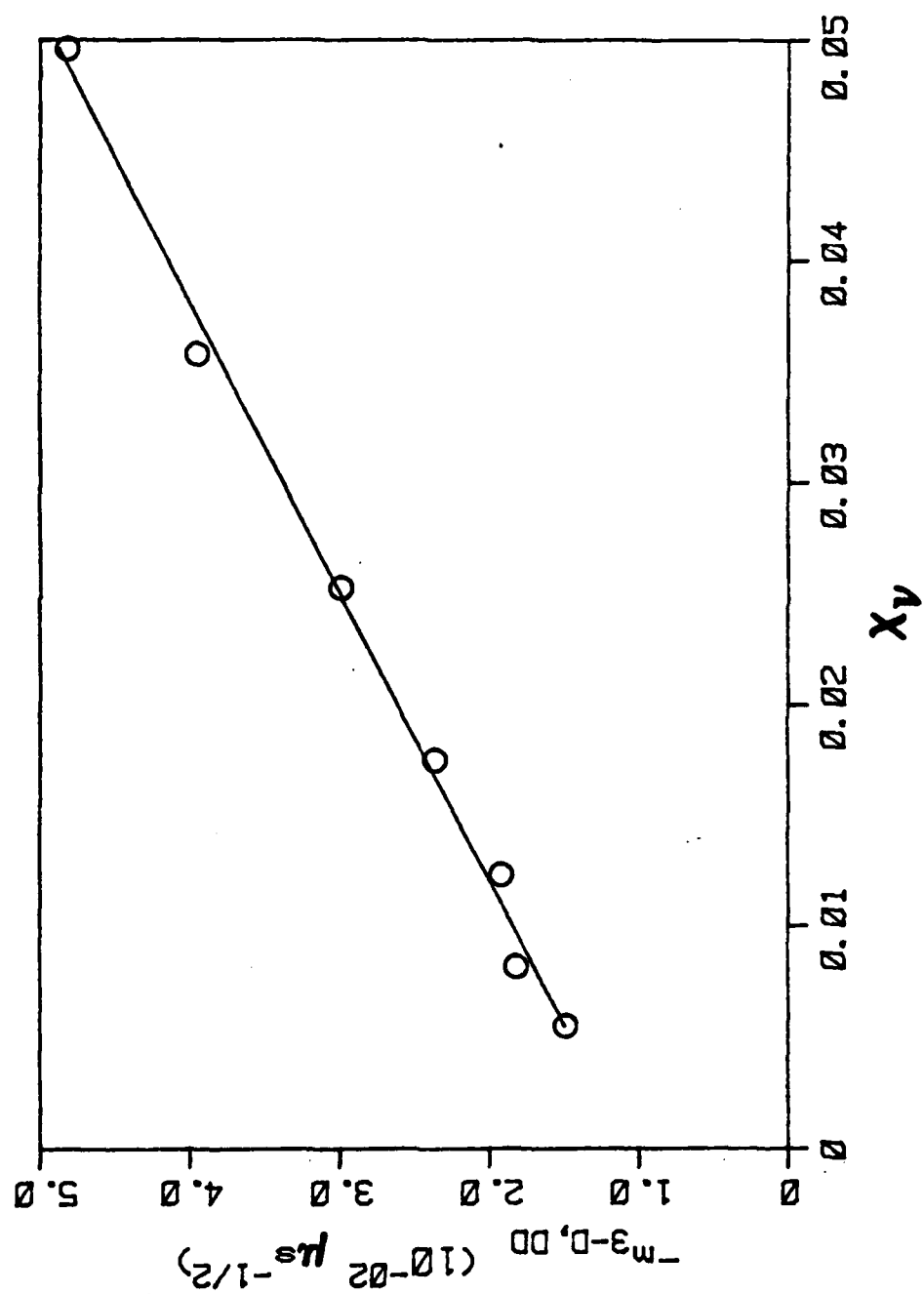
Fig. 8 The guest emission linewidth (fwhm) normalized by Γ vs. the interaction volume n . From bottom to top, these curves are for guest mole fractions $p = 1.0$, 0.5 , 0.2 and 0.1 respectively.

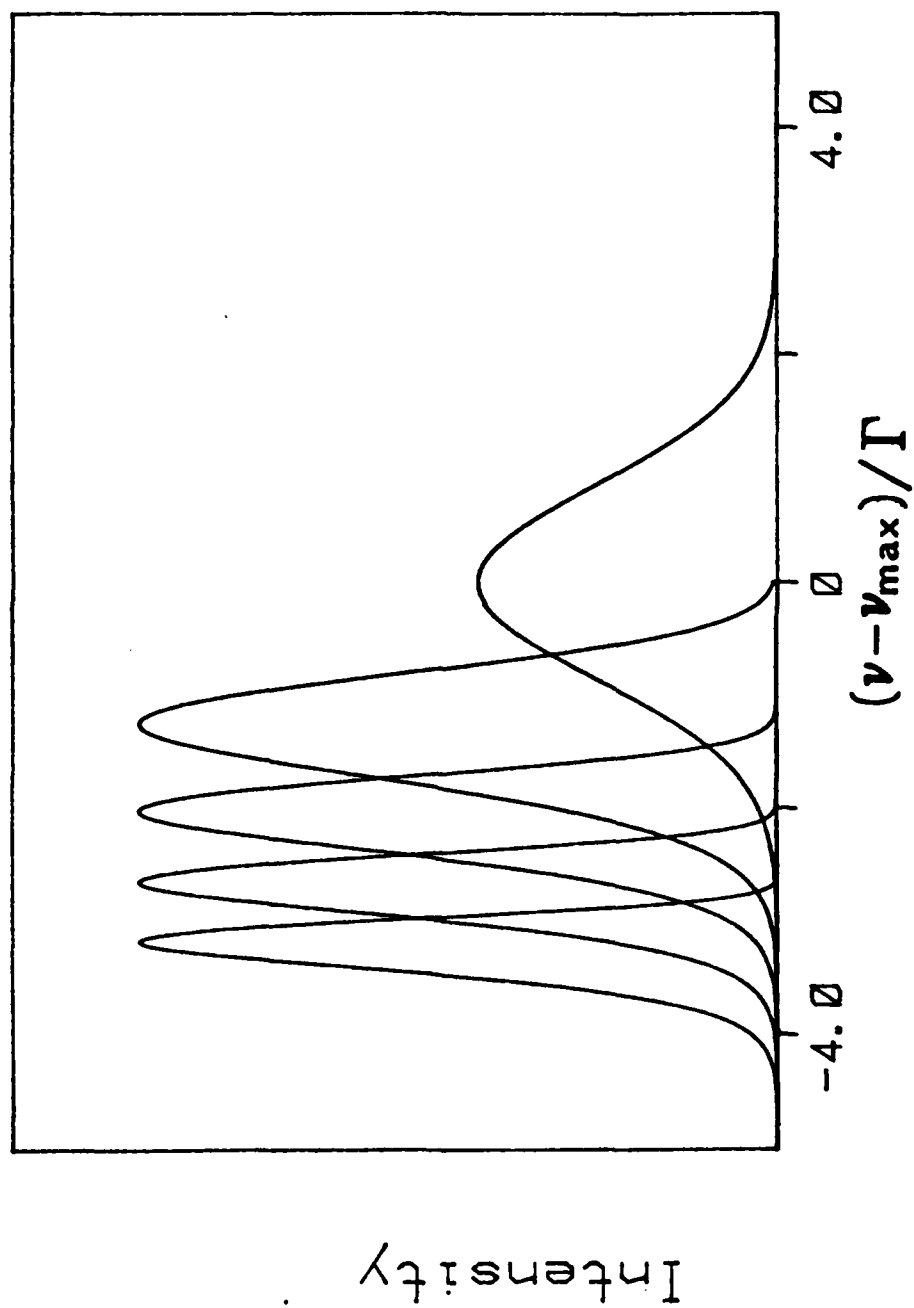


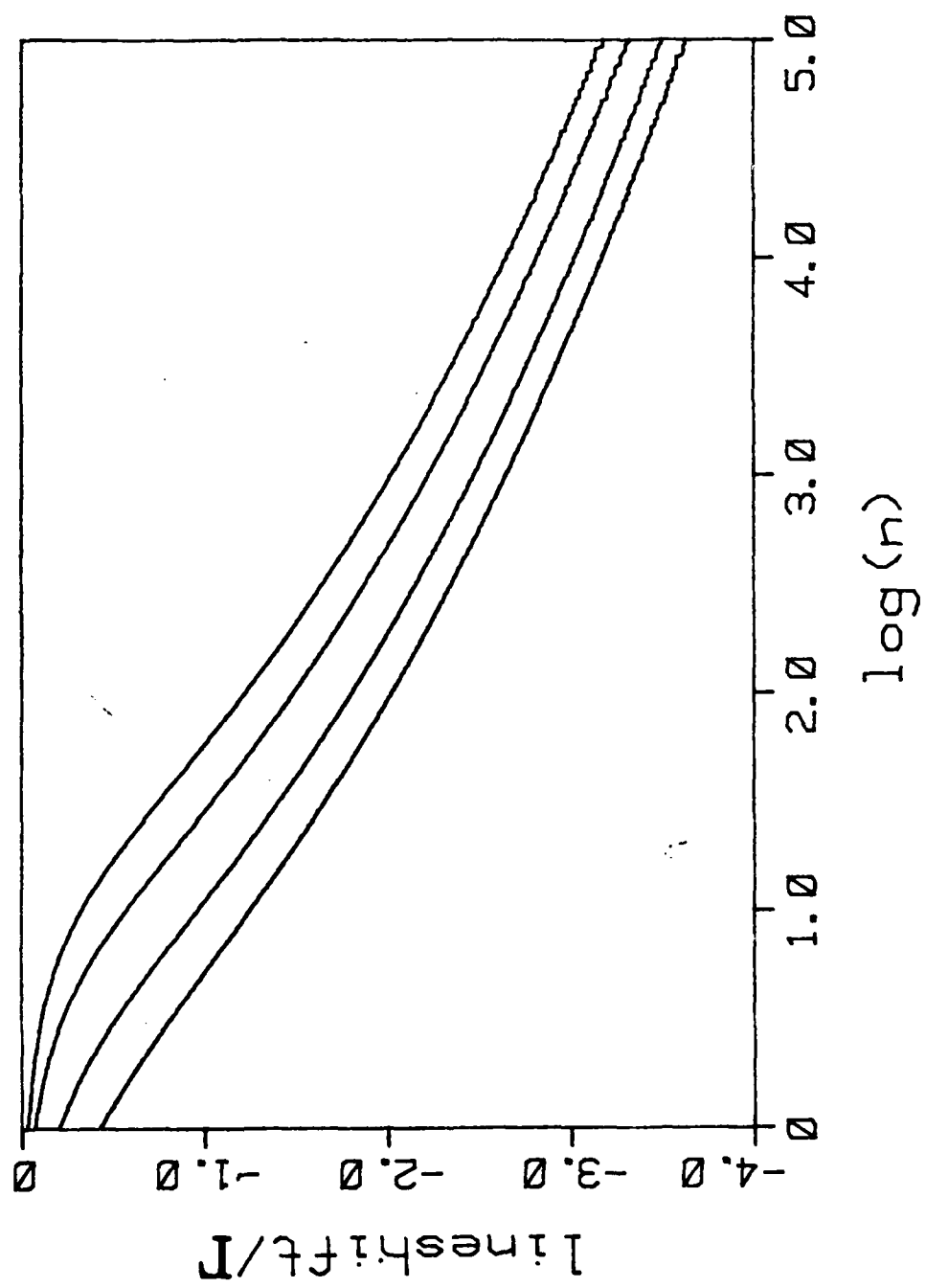


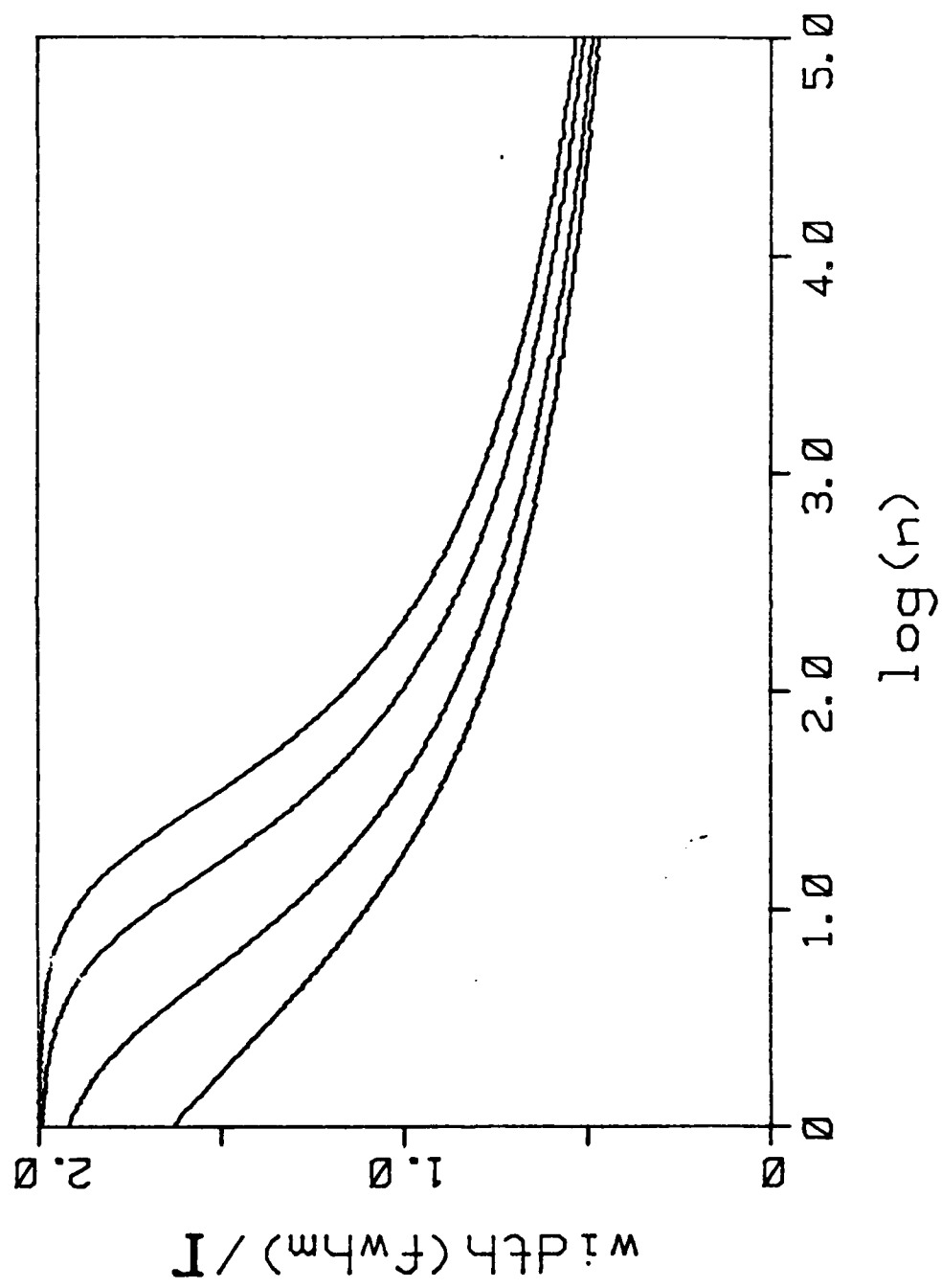












TECHNICAL REPORT DISTRIBUTION LIST, GEN

	<u>No. Copies</u>		<u>No. Copies</u>
Office of Naval Research Attn: Code 413 800 North Quincy Street Arlington, Virginia 22217	2	Naval Ocean Systems Center Attn: Mr. Joe McCartney San Diego, California 92152	1
ONR Pasadena Detachment Attn: Dr. R. J. Marcus 1030 East Green Street Pasadena, California 91106	1	Naval Weapons Center Attn: Dr. A. B. Amster, Chemistry Division China Lake, California 93555	1
Commander, Naval Air Systems Command Attn: Code 310C (H. Rosenwasser) Department of the Navy Washington, D.C. 20360	1	Naval Civil Engineering Laboratory Attn: Dr. R. W. Drisko Port Hueneme, California 93401	1
Defense Technical Information Center Building 5, Cameron Station Alexandria, Virginia 22314	12	Dean William Tolles Naval Postgraduate School Monterey, California 93940	1
Dr. Fred Saalfeld Chemistry Division, Code 6100 Naval Research Laboratory Washington, D.C. 20375	1	Scientific Advisor Commandant of the Marine Corps (Code RD-1) Washington, D.C. 20380	1
U.S. Army Research Office Attn: CRD-AA-IP P. O. Box 12211 Research Triangle Park, N.C. 27709	1	Naval Ship Research and Development Center Attn: Dr. G. Bosmajian, Applied Chemistry Division Annapolis, Maryland 21401	1
Mr. Vincent Schaper DTNSRDC Code 2803 Annapolis, Maryland 21402	1	Mr. John Boyle Materials Branch Naval Ship Engineering Center Philadelphia, Pennsylvania 19112	1
Naval Ocean Systems Center Attn: Dr. S. Yamamoto Marine Sciences Division San Diego, California 91232	1	Mr. A. M. Anzalone Administrative Librarian PLASTEC/ARRADCOM Bldg 3401 Dover, New Jersey 07801	1

TECHNICAL REPORT DISTRIBUTION LIST, 051A

	<u>No. Copies</u>		<u>No. Copies</u>
Dr. M. A. El-Sayed Department of Chemistry University of California, Los Angeles Los Angeles, California 90024	1	Dr. M. Rauhut Chemical Research Division American Cyanamid Company Bound Brook, New Jersey 08805	1
Dr. E. R. Bernstein Department of Chemistry Colorado State University Fort Collins, Colorado 80521	1	Dr. J. I. Zink Department of Chemistry University of California, Los Angeles Los Angeles, California 90024	1
Dr. C. A. Heller Naval Weapons Code 6059 China Lake, California 93555	1	Dr. D. M. Burland IBM San Jose Research Center 5600 Cottle Road San Jose, California 95143	1
Dr. J. R. MacDonald Chemistry Division Naval Research Laboratory Code 6110 Washington, D.C. 20375	1	Dr. John Cooper Code 6130 Naval Research Laboratory Washington, D.C. 20375	1
Dr. G. B. Schuster Chemistry Department University of Illinois Urbana, Illinois 61801	1	Dr. William M Jackson Department of Chemistry Howard University Washington, D.C. 20059	1
Dr. A. Adamson Department of Chemistry University of Southern California Los Angeles, California 90007	1	Dr. George E. Walrafen Department of Chemistry Howard University Washington, D.C. 20059	1
Dr. M. S. Wrighton Department of Chemistry Massachusetts Institute of Technology Cambridge, Massachusetts 02139	1	Dr. Joe Brandelik AFWAL/AADO-1 Wright Patterson AFB Fairborn, Ohio 45433	1
Dr. A. Paul Schaap Department of Chemistry Wayne State University Detroit, Michigan 49207	1	Dr. Gary Bjorklund IBM 5600 Cottle Road San Jose, California 95143	1
		Dr. Carmen Ortiz Cousejo Superior de Investigaciones Cientificas Serrano 117 Madrid 6, Spain	1

END

FILMED

9-83

DTIC